Differential nucleosome occupancy modulates alternative splicing in Arabidopsis thaliana

Jabre, I., Chaudhary, S., Guo, W., Kalyna, M., Reddy, A. S. N., Chen, W., Zhang, R., Wilson, C. and Syed, N.

New Phytologist

Differential nucleosome occupancy modulates alternative splicing in Arabidopsis thaliana

Journal:	*New Phytologist*
Manuscript ID	NPH-RAP-2020-34391.R1
Manuscript Type:	RAP - Rapid Report
Date Submitted by the Author:	n/a
Key Words:	Alternative Splicing, Cold Stress, Nucleosome Positioning, Exitrons, Co-transcriptional Splicing, Arabidopsis thaliana

Complete List of Authors:
Jabre, Ibtissam ; Canterbury Christ Church University, Human and Life Sciences
Chaudhary, Saurabh; Cardiff University, School of Biosciences
Guo, Wenbin; The James Hutton Institute, Informatics and Computational Sciences
Kalyna, Maria; University of Natural Resources and Life Sciences, Department of Applied Genetics and Cell Biology
REddy, Anireddy; Colorado State University, Department of Biology and Program in Cell and Molecular Biology
Chen, Weizhong; Cornell University, Department of Molecular Biology and Genetics
Zhang, Runxuan; James Hutton Institute, Informatics and Computational Sciences; The James Hutton Institute
Wilson, Cornelia; Canterbury Christ Church University, Human and Life Sciences
Syed, Naeem; Canterbury Christ Church University, Human and Life Sciences;

Differential nucleosome occupancy modulates alternative splicing in *Arabidopsis thaliana*

Ibtissam Jabre[1*6], Saurabh Chaudhary[1*7], Wenbin Guo[3], Maria Kalyna[2], Anireddy S N Reddy[4], Weizhong Chen[5], Runxuan Zhang[3], Cornelia Wilson[1] and Naeem H Syed[1]

[1]School of Human and Life Sciences, Canterbury Christ Church University, Canterbury, CT1 1QU, UK.
[2]Department of Applied Genetics and Cell Biology, University of Natural Resources and Life Sciences - BOKU, Muthgasse 18, 1190 Vienna, Austria.
[3]Computational Sciences, The James Hutton Institute, Dundee DD2 5DA, UK.
[4]Department of Biology and Program in Cell and Molecular Biology, Colorado State University, Fort Collins, CO 80523-1878, USA.
[5]Department of Molecular Biology & Genetics, Cornell University, Ithaca, NY 14853-2703, USA.
[6]School of Biosciences and Medicine, University of Surrey, Guildford GU2 7XH, UK.
[7]Cardiff School of Biosciences, Cardiff University, Cardiff, CF10 3AX, UK.

*Contributed equally
Corresponding author: Naeem Syed, Canterbury Christ Church University, Canterbury, CT1 1QU; phone +44 1227 782511; Email: naeem.syed@canterbury.ac.uk

Introduction: 618 words
Materials and Methods: 297 words
Results: 1424 words
Discussion: 806 words
Figures: Four coloured
Tables: NIL
Supporting Information: Nine files

Summary

- Alternative splicing (AS) is a major gene regulatory mechanism in plants. Recent evidence supports co-transcriptional splicing in plants, hence the chromatin state can impact AS. However, how dynamic changes in the chromatin state such as nucleosome occupancy influence the cold-induced AS remains poorly understood.
- Here, we generated transcriptome (RNA-Seq) and nucleosome positioning (MNase-Seq) data for *Arabidopsis thaliana* to understand how nucleosome positioning modulates cold-induced AS.
- Our results show that characteristic nucleosome occupancy levels are strongly associated with the type and abundance of various AS events under normal and cold temperature conditions in Arabidopsis. Intriguingly, exitrons, alternatively spliced internal regions of protein-coding exons, exhibit distinctive nucleosome positioning pattern compared to other alternatively spliced regions. Likewise, nucleosome patterns differ between exitrons and retained introns pointing to their distinct regulation.
- Collectively, our data show that characteristic changes in nucleosome positioning modulate AS in plants in response to cold.

Key words: Alternative Splicing, *Arabidopsis thaliana*, Cold Stress, Co-transcriptional Splicing, Exitrons, Nucleosome Positioning.

Introduction

Plants employ different strategies to control their transcriptional program during the daily cycles of light-dark and in response to environmental stress to confer adaptive responses (Zhu, 2016; Laloum *et al.*, 2017; Lämke & Bäurle, 2017). Recent evidence shows that alternative splicing (AS) regulation is a key gene regulatory mechanism in plants (Calixto *et al.*, 2018; Filichkin *et al.*, 2018; Jabre *et al.*, 2019). In plants and animals, AS is regulated co-transcriptionally (Brody *et al.*, 2011; Tilgner *et al.*, 2012; Li *et al.*, 2020; Zhu *et al.*, 2020). RNA polymerase II (RNAPII) speed during transcription may be affected by the chromatin state that in turn determines AS outcomes (Alexander *et al.*, 2010; Ullah *et al.*, 2018; Zhu *et al.*, 2018). Emerging evidence shows that the chromatin environment has a strong bearing on the splicing process by modulating RNAPII processivity and splicing factors (SFs) recruitment (Nojima *et al.*, 2018; Jabre *et al.*, 2019; Kindgren *et al.*, 2019; Li *et al.*, 2020; Yu *et al.*, 2019; Zhu *et al.*, 2020). Recent native elongating transcript sequencing (NET-Seq) and global run-on sequencing (GRO-Seq) studies from mammals and *Arabidopsis thaliana* (hereafter Arabidopsis) show that phosphorylation of RNAPII C-terminal domain mediates interactions with the spliceosome and that RNAPII accumulation is associated with different chromatin states (Nojima *et al.*, 2018; Zhu *et al.*, 2018). Remarkably, sequencing of the chromatin-bound nascent RNAs in Arabidopsis revealed that almost all introns are spliced co-transcriptionally and the efficiency of intron removal is more robust in protein-coding genes than noncoding RNAs (Li *et al.*, 2020). Furthermore, it was also demonstrated that co-transcriptional splicing (CTS) efficiency is dependent on the number of exons but not gene length (Zhu *et al.*, 2020). Therefore, appropriate exon-intron definition may be important for CTS in Arabidopsis (Li *et al.*, 2020). For example, nucleosome occupancy was found to be higher on exons and also accompanied by a higher level of RNAPII (Chodavarapu *et al.*, 2010). Therefore, higher nucleosome occupancy on exons is intrinsically associated with exon definition, RNAPII processivity and splicing kinetics (Jabre *et al.*, 2019). Previously, it has been demonstrated that change in RNAPII speed in both directions can influence splicing factor recruitment and splicing efficiency (Dujardin *et al.*, 2014; Godoy Herz *et al.*, 2019; Leng *et al.*, 2020). Therefore, nucleosome positioning may modulate different AS events and their ratios under variable growth and/or stress conditions to alter intron/exon boundaries and provide a context through which AS patterns could be modulated (Jabre *et al.*, 2019). For example, RNAi lines of a chromatin remodeler gene (*ZmCHB101*) in maize showed altered nucleosome density, RNAPII elongation rate, and changes in splicing patterns under osmotic stress (Yu *et al.*, 2019).

Similarly, widespread nucleosome remodelling in rice, as a result of phosphate starvation and cold stress, was associated with differential gene expression (Roy *et al.*, 2014; Zhang *et al.*, 2018). Since cold can influence the RNAPII elongation kinetics in Arabidopsis (Kindgren *et al.*, 2019), we reasoned that rapid cold-induced alternative splicing response in Arabidopsis (Calixto *et al.*, 2018) may be associated with nucleosome remodelling. Henceforth, we used cold treatment as a system of choice to investigate whether it could modulate nucleosome positioning and influence AS.

We performed RNA-Seq and micrococcal nuclease sequencing (MNase-Seq) for Columbia wild type (Col-0) accession of Arabidopsis growing at normal temperature (22^{o}C) and under cold stress (4^{o}C) for 24 hours. We observed genome-wide changes in AS and gene expression between Col-0_22^{o}C and Col-0_4^{o}C plants. Our results show that temperature-dependent differences in nucleosome positioning are sufficient to modulate different types of AS events and their abundance. Remarkably, exitrons, alternatively spliced internal regions of protein-coding exons (Marquez *et al.*, 2015), can also be distinguished from flanking exons by distinctive nucleosome occupancy to facilitate their recognition by the splicing machinery.

Materials and Methods

The detailed experimental procedure is provided in the supplementary information file (Supporting Information Method S1). Briefly, leaf tissues were harvested from three weeks old Col-0 plants grown at 22°C and cold treated (4°C) for 24 h. Total RNA and nucleosome bound genomic DNA (gDNA) were extracted for Illumina paired-end sequencing using RNA extraction and Qiagen DNA kits, respectively. The raw reads generated from RNA-Seq and MNase-Seq experiments were quality checked using Trimmomatic (Bolger *et al.*, 2014). The high quality reads from RNA-Seq experiment were used to quantify the transcripts expression using Salmon v0.82 (Patro *et al.*, 2017) and AtRTD2-QUASI (Zhang *et al.*, 2017) as reference. Differential Expressed Genes (DEGs) and differential alternatively spliced (DAS) genes were identified using 3D-RNA-Seq pipeline as described previously by (Calixto *et al.*, 2018; Guo *et al.*, 2019). Gene functional enrichment analysis was performed using DAVID v6.8 (Huang *et al.*, 2009a,b). The gene ontology (GO) terms were assigned to DEGs and DAS genes with FDR ≤0.05. AS events, AS event inclusion level (Percent Spliced In – PSI indicates how efficiently sequences of interest are spliced into transcripts) and the difference in this inclusion (ΔPSI) between Col-0 grown at 22^{o}C and 4^{o}C were identified using SUPPA2 (Alamancos *et al.*, 2015; Trincado *et al.*, 2018). Only AS events having a *p*-value ≤0.05 are identified as DAS events.

For MNase-Seq high quality reads were mapped to the TAIR10 Arabidopsis reference genome using Bowtie v1.2.2 (Langmead *et al.*, 2009) with "-m" set to 1 to output only uniquely mapped reads. Improved Nucleosome-Positioning Algorithm (iNPS) was used for accurate genome-wide nucleosome positioning as described previously by (Chen *et al.*, 2014). Differential Nucleosome Positioning (DNP) analysis was performed using DANPOS v2.1.2 (Chen *et al.*, 2013). Nucleosome signals were plotted around different genomic regions using deepTools v3.5.0 (Ramírez *et al.*, 2014).

Results

Cold-regulated DE and DAS genes affect different biological processes

In Arabidopsis, nucleosome positioning differentially marks promoter regions, gene bodies as well as exons and introns, indicating a potential link of chromatin architecture to gene expression and splicing regulation (Chodavarapu *et al.*, 2010). To investigate if cold-induced AS in Arabidopsis is regulated by nucleosome occupancy, we performed RNA-Seq and MNase-Seq of Col-0 lines before and after a shift from 22°C to 4°C for 24 hours. Using the previously published 3D-RNA-Seq pipeline (Calixto *et al.*, 2018; Guo *et al.*, 2019) (Supporting Information Method S1), we identified 6252 DEGs and 2283 DAS genes. Of the 6252 DEGs, 3323 were up-regulated and 2929 were down-regulated (Table S1). We observed that most transcriptional changes are associated with genes that do not display splicing changes (70.5% DE only genes). Similarly, a large proportion of splicing changes occur in genes that are not differentially expressed (19.3% DAS only genes). The overlap of DEGs and DAS genes is significant (10.2%; hypergeometric test, $p < 1.222e^{-39}$) (Fig. 1a), suggesting that cold stress modulates both transcriptional and AS responses of some genes, which is in line with previously published reports from Arabidopsis (Calixto *et al.*, 2018). Gene functional enrichment analysis of DEGs showed significant (FDR <0.05) enrichment in diverse biological functions including circadian rhythm, cold stress, and photosynthesis regulation. Cellular components terms enrichment for DEGs were mainly for plasma membrane, and vacuole (Fig. S1a). DAS genes showed significant (FDR <0.05) enrichment in mRNA processing, RNA splicing and protein phosphorylation, whereas those of cellular components and molecular functions were mainly enriched in the nucleus and mRNA/ATP/protein binding activities, respectively (Fig. S1b). To identify AS events regulated by cold stress, we analysed RNA-Seq data using SUPPA2 (Supporting Information Method S1) (Alamancos *et al.*, 2015; Trincado *et*

al., 2018). We identified 3032 cold-regulated AS events that showed significant (*p*-value <0.05) changes in the ΔPSI index (see Methods) distributed within different types of AS events. Changes in intron retention (IR) events are the most prevalent, followed by usage of alternative acceptor (A3'SS) and alternative donor (A5'SS) sites, exon skipping (ES), and exitrons (EIs) (Table S2, S3; Fig. 1b; Fig. S2). EIs are alternatively spliced internal regions of protein-coding exons (Marquez *et al.*, 2015; Staiger & Simpson, 2015; Sibley *et al.*, 2016). At least 6.6% of Arabidopsis and 3.7% of human protein-coding genes contain exitrons (Marquez *et al.*, 2015; Zhang *et al.*, 2017). Due to their distinctive features, we grouped EIs separately from IR events.

Nucleosome occupancy modulates variety and abundance of alternative splicing events

To investigate how nucleosome occupancy modulates splicing, we performed nucleosome positioning and DNP analysis (Supporting Information Method S1). We detected 19233 significant Differential Positioned Nucleosomes (DPNs) upon shifting plants from 22°C to 4°C for 24 hours that were significantly (Supporting Information Method S1) associated with 7357 genes (Tables S4, S5, and S6). Interestingly, 833 (9.5%) (hypergeometric test, $p < 1.498e^{-24}$) cold-induced DAS genes displayed changes in nucleosome occupancy (Fig. 1c). We first profiled nucleosome occupancy across exons and flanking regions, where we could detect a significant drop of nucleosome occupancy signals at 4°C around exons and flanking regions (one-tailed *t* test, *p* <0.0001) (Fig. S3). Then, we sought if changes in nucleosome occupancy around the splice site can modulate different AS events. For that, we profiled nucleosome signals of 3032 cold-regulated DAS events that showed significant (*p*-value <0.05) ΔPSI values upon cold stress. Interestingly, different DAS events displayed significant changes in nucleosome occupancy signals around the donor and acceptor sites of different AS events at 22°C and 4°C (One-way ANOVA-test, *p* <0.01, Fig 2a). We also could detect an overall drop of nucleosome occupancy level for all AS events upon cold stress. For example, nucleosome occupancy is relatively higher for ES event at 22°C compared to 4°C (One-tailed *t* test, *p* <0.0001, Fig 2a) potentially impacting exon definition and loss of exons from different transcripts (Fig. 2a). Since nucleosome occupancy levels differentially associate with various types of AS events between plants grown at different temperatures, we sought to explore if this relationship holds true to explain the ratios of these AS events. For that, we grouped PSI values (see Methods) for different AS events detected in plants grown at both temperature conditions into four bins and aligned nucleosome peaks 200 base pairs (bp) upstream and downstream the

exon (or intron) for which the PSI value was calculated. It is notable that for ES, A3'SS and A5'SS, alternative regions with higher inclusion levels (higher PSI values) display more nucleosome occupancy across the splice sites, whereas IRs with higher inclusion levels display less nucleosome occupancy across the splice sites (One-way ANOVA-test, p <0.001, Fig 2.b). Collectively, the differences in nucleosome occupancy levels detected for plants grown at different temperatures for different AS events or for the same PSI group within the same AS event show that alternative regions involved in different types of AS events may be associated with specific epigenetic features potentially influencing local splicing events and abundance of transcripts.

Nucleosome occupancy is strongly associated with negative or positive AS regulation

Next, we interrogated how nucleosome occupancy levels, for the same set of genes, differ between DAS and non-DAS genes under normal and cold conditions. For that, we profiled nucleosome occupancy levels across the exons of DAS and non-DAS genes. We found relatively lower nucleosome occupancy for DAS compared to non-DAS exons at 22^{o}C and as well as 4^{o}C (One-tailed t test, p <0.0001, Fig. 3a). Since nucleosome occupancy globally drops under cold conditions, we sought to investigate how nucleosome occupancy would correlate with splice junctions affected differently by cold stress. Therefore, we grouped the SJs of the AS events (p-value < 0.05) obtained from SUPPA based on their ΔPSI value to obtain positively, negatively, and unaffected SJs (Supporting Information Method S1). Interestingly, cold stress positively regulates 1208 SJs, negatively regulates 1054, and leaves 673 SJs un-affected. (Fig. 3b; Table S7), This data strongly supports previous data showing that cold-stress induced AS in plants (Calixto *et al.*, 2018). To profile nucleosome occupancy around these SJs, we plotted nucleosome density of negatively-, positively-affected, and unaffected SJs for Col-0 grown at 22^{o}C and 4^{o}C (Fig. 3c). Remarkably, nucleosome profiles of unaffected SJs for both, the donor and acceptor site are significantly different compared to negatively or positively affected SJs at both temperatures (One-way ANOVA, p <0.01, Fig. 3C). Additionally, we also detected a significant association between negatively and positively affected SJs with regions associated with DNPs (Fisher exact test, p-value <0.001). Overall, our results show that changes in nucleosome occupancy levels across intron-exon junctions and exons are likely to regulate splice site selection and subsequently modulate splicing regulation in both positive and negative manner.

Characteristic nucleosome occupancy patterns define exitrons

EIs have a lower guanine-cytosine (GC) content than adjacent sequences of EI-containing exons (Marquez *et al.*, 2015). Therefore, we asked whether differential GC content in EI sequences is associated with nucleosome occupancy to distinguish them from flanking exonic regions. To answer this, we profiled nucleosome occupancy across ~2400 EIs identified in Arabidopsis (Marquez *et al.*, 2015; Zhang *et al.*, 2017) and 500 bp upstream and downstream from their starts and ends. We found sharp peaks of nucleosome occupancy located before the start and after the end of EIs and slightly lower occupancy in the middle of EIs, which is different from nucleosome patterns observed across exons (Fig. S3). Additionally, we detected a decrease of nucleosome occupancy across exitrons under cold stress (One-tailed *t* test, $p < 0.0001$, Fig. 4a). Comparison of nucleosome occupancy levels over EIs grouped into four bins according to the PSI values showed that higher exitron inclusion correlates with higher nucleosome occupancy and showed variable levels under normal and cold conditions (Fig. 4b), hence pointing towards their regulation under cold stress. This pattern differs from the one observed for IRs, where IRs with higher inclusion levels display less nucleosome occupancy (Fig. 2b). Interestingly, in this respect, EIs are more similar to ES, A5'SS and A3'SS events due to their exonic features (Fig. 2b). Since EIs have a higher GC content than IRs and constitutive introns (Marquez *et al.*, 2015), we compared their nucleosome profiles in normal and cold conditions. We observed that nucleosome occupancy levels are higher for EIs compared to IRs at 22^{o}C and 4^{o}C (One-way ANOVA, $p < 0.0001$, Fig. 4c). This implies that chromatin structure plays different roles in the definition and splicing of IRs and EIs. Overall, these results revealed the importance of nucleosome occupancy in defining EIs and their distinction from IRs to regulate their AS profiles under normal and cold conditions.

Discussion

Recent evidence from Arabidopsis shows that transcription and splicing are largely coupled (Dolata *et al.*, 2015; Hetzel *et al.*, 2016; Ullah *et al.*, 2018; Jabre *et al.*, 2019; Jia *et al.,* 2020), and that epigenetic features in plants regulate transcriptional activity and differentially mark exons and introns (Zhu *et al.*, 2018). Not surprisingly, very recent studies employing sequencing of chromatin-bound RNAs reveal that almost all introns in Arabidopsis are spliced

co-transcriptionally (Li *et al.*, 2020). Furthermore, RNAPII elongation speed has been found to be slower in nucleosome-rich exons allowing more time for the splicing process to take place (Chodavarapu *et al.*, 2010; Zhu *et al.*, 2018). However, how the chromatin environment influences different types of AS events and their ratios under variable growth and stress conditions remains elusive in plants. Since splicing/AS regulation is achieved by the context of the *cis*-regulatory sequences as well as the chromatin environment (Reddy *et al.*, 2013), it is important to understand the relative contributions of epigenetic landscapes. In this study, using Arabidopsis Col-0 ecotype plants, we demonstrate that cold-induced DAS is accompanied by changes in nucleosome occupancy levels. Although nucleosome occupancy falls globally under cold conditions in Arabidopsis; nonetheless, nucleosome profiles around intron/exon boundaries among different PSI groups, negatively and positively affected AS events displayed characteristic patterns. Further work is needed to understand how variable nucleosome occupancy modulates RNAPII processivity and alternative splicing in plants. However, since nucleosome occupancy and RNAPII density has a close relationship in Arabidopsis (Chodavarapu *et al.*, 2010), it is likely that chromatin architecture plays a similar role in plants and animals as progesterone treated breast cancer cells displayed weaker nucleosome densities and lower RNAPII accumulation, resulting in alteration in splice site recognition and exon skipping (Iannone *et al.*, 2015). Since histone modification modulate AS in humans (Luco *et al.*, 2010), similar mechanism also may modulate splicing variation in plants. Intriguingly, exitrons also show distinctive nucleosome occupancy (Fig. 4), which may help to differentiate them from flanking exonic regions. Furthermore, despite their classification as a group of IR, exitrons display different nucleosome patterns compared to retained introns; pointing to their distinct regulation.

We propose that these changes in nucleosome occupancy may provide the basic definition to exons and introns to coordinate RNAPII processivity. However, it is apparent that the splicing process is also fine-tuned by various *trans*-regulatory factors and histone modifications under variable growth and stress conditions (Kindgren *et al.*, 2019; Zhu *et al.*, 2020). Our data support this notion and it is likely that higher nucleosome occupancy may regulate RNAPII accumulation around splice sites and enable SFs recruitment to facilitate and/or modulate splicing variation. Interestingly, RNAPII elongation speed in Arabidopsis would be much slower after clearing a 3'SS and towards the end of an exon, and may not provide sufficient time (because of higher speed in plant introns) for RNAPII to recognise the 5'SS (Kindgren *et al.*, 2019). Furthermore, recent findings show that RNAPII accumulates upstream of the 5'SS,

potentially to provide additional time/checkpoint to regulate splicing in mammals and plants (Kindgren *et al.*, 2019; Nojima *et al.*, 2015). Therefore, variation in nucleosome occupancy with an additional peak just after 5'SS (Fig. 3a) may mediate RNAPII accumulation and influence CTS (Nojima *et al.*, 2015; Kindgren *et al.*, 2019). Arguably, this is why 5'SS splicing dynamics are much more complicated and the scanning splicing machinery has to travel to the branch point/ polypyrimidine tract to complete lariat formation and process 5'SS. Beggs and colleagues proposed, the initial propensity of splicing is low but increases subsequently to allow accumulation of splicing precursors to improve splicing efficiency in subsequent and/or successive reactions (Aitken *et al.*, 2011). These findings are in broad agreement with CTS in Arabidopsis as the CTS process is more efficient in genes with multiple introns/exons and is independent of the gene length (Zhu *et al.*, 2020). Mutations at the 3'SS and 5'SS impact transcription initiation and a mutant 3'SS reduces the first step of CTS in yeast (Aitken *et al.*, 2011). Similarly, splicing dynamics of the human beta-globin gene which fails to form lariat formation and complete 5'SS when a deletion removes the polypyrimidine tract and AG dinucleotide at the 3'SS (Reed & Maniatis, 1985). Therefore, it is tempting to speculate that nucleosome occupancy and/or histone decorations may be more important in the 5' regions of exons providing a checkpoint to the elongating RNAPII to help recognise 5'SS, form lariat and cleave at the 5'SS and 3'SS. It is evident that efficient splicing/AS is dependent on an optimum RNAPII elongation speed and any variation (slow or fast) results in changes in splicing patterns in humans and plants (Dujardin *et al.*, 2014; Godoy Herz *et al.*, 2019; Leng *et al.*, 2020).

Collectively our data points towards the importance of epigenetic features such as nucleosome occupancy for plants grown under different and recurrent growth and stress conditions.

Funding

We thank the funding agencies for research support. Leverhulme Trust [RPG-2016-014]; DOE Office of Science, Office of Biological and Environmental Research (BER) [DE-SC0010733]; National Science Foundation and the US Department of Agriculture (ASNR); Austrian Science Fund (FWF) for MK [P26333]. Funding for open access charge: Leverhulme

Availability of Data and Materials

All RNA-Seq and MNase-Seq raw data generated in this work is submitted to NCBI-SRA under the accession number "PRJNA592356".

Supplemental Information

Supplemental Information is available at New Physiologist online.

References

Aitken S, Alexander RD, Beggs JD. **2011**. Modelling reveals kinetic advantages of co-transcriptional splicing. *PLoS Computational Biology* **7**: e1002215.

Alamancos GP, Pagès A, Trincado JL, Bellora N, Eyras E. **2015**. Leveraging transcript quantification for fast computation of alternative splicing profiles. *RNA* **21**: 1521-1531.

Alexander RD, Innocente SA, Barrass JD, Beggs JD. **2010**. Splicing-Dependent RNA polymerase pausing in yeast. *Molecular Cell* **40**: 582-593.

Bolger AM, Lohse M, Usadel B. **2014**. Trimmomatic: A flexible trimmer for Illumina sequence data. *Bioinformatics* **30**: 2114–2120.

Brody Y, Neufeld N, Bieberstein N, Causse SZ, Böhnlein EM, Neugebauer KM, Darzacq X, Shav-Tal Y. **2011**. The in vivo kinetics of RNA polymerase II elongation during co-transcriptional splicing. *PLoS Biology* **9**: e1000573.

Calixto CPG, Guo W, James AB, Tzioutziou NA, Entizne JC, Panter PE, Knight H, Nimmo HG, Zhang R, Brown JWS. **2018**. Rapid and dynamic alternative splicing impacts the arabidopsis cold response transcriptome[CC-BY]. *Plant Cell* **30**: 1424-1444.

Chen W, Liu Y, Zhu S, Green CD, Wei G, Han JDJ. **2014**. Improved nucleosome-positioning algorithm iNPS for accurate nucleosome positioning from sequencing data. *Nature Communications* **18**: 4909-4923.

Chen K, Xi Y, Pan X, Li Z, Kaestner K, Tyler J, Dent S, He X, Li W. **2013**. DANPOS: Dynamic analysis of nucleosome position and occupancy by sequencing. *Genome Research* **23**: 341–351.

Chodavarapu RK, Feng S, Bernatavichute Y V., Chen PY, Stroud H, Yu Y, Hetzel JA, Kuo F, Kim J, Cokus SJ, *et al.* 2010. Relationship between nucleosome positioning and DNA methylation. *Nature* **466**: 388-392.

Dolata J, Guo Y, Ko owerzo A, Smolinski D, Brzyzek G, Jarmo owski A, Swiezewski S. **2015**. NTR1 is required for transcription elongation checkpoints at alternative exons in Arabidopsis. *The EMBO Journal* **34**: 544–558.

Dujardin G, Lafaille C, de la Mata M, Marasco LE, Muñoz MJ, Le Jossic-Corcos C, Corcos L, Kornblihtt AR. **2014**. How slow RNA Polymerase II elongation favors alternative exon skipping. *Molecular Cell* **54**: 683–690.

Filichkin SA, Hamilton M, Dharmawardhana PD, Singh SK, Sullivan C, Ben-Hur A, Reddy ASN, Jaiswal P. **2018**. Abiotic stresses modulate landscape of poplar transcriptome via alternative splicing, differential intron retention, and isoform ratio switching. *Frontiers in Plant Science* **9**: 5-22.

Godoy Herz MA, Kubaczka MG, Brzyżek G, Servi L, Krzyszton M, Simpson C, Brown J, Swiezewski S, Petrillo E, Kornblihtt AR. **2019**. Light regulates plant alternative splicing through the control of transcriptional elongation. *Molecular Cell* **73**: 1066-1074.

Hetzel J, Duttke SH, Benner C, Chory J. **2016**. Nascent RNA sequencing reveals distinct features in plant transcription. *Proceedings of the National Academy of Sciences* **113**: 12316-12321.

Huang DW, Sherman BT, Lempicki RA. **2009a**. Systematic and integrative analysis of large gene lists using DAVID bioinformatics resources. *Nature Protocols* **4**: 44–57.

Huang DW, Sherman BT, Lempicki RA. **2009b**. Bioinformatics enrichment tools: Paths toward the comprehensive functional analysis of large gene lists. *Nucleic Acids Research* **37**: 1–13.

Iannone C, Pohl A, Papasaikas P, Soronellas D, Vicent GP, Beato M, Valcárcel J. **2015**. Relationship between nucleosome positioning and progesterone-induced alternative splicing in breast cancer cells. *RNA* **21**: 360-374.

Jabre I, Reddy ASN, Kalyna M, Chaudhary S, Khokhar W, Byrne LJ, Wilson CM, Syed NH. **2019**. Does co-transcriptional regulation of alternative splicing mediate plant stress responses? *Nucleic acids research* **47**: 2716-2726.

Kindgren P, Ivanov M, Marquardt S. **2019**. Native elongation transcript sequencing reveals temperature dependent dynamics of nascent RNAPII transcription in Arabidopsis **48**: 2332-2347.

Laloum T, Martín G, Duque P. **2017**. Alternative splicing control of abiotic stress responses. *Trends in Plant Science* **23**: 140-150.

Lämke J, Bäurle I. **2017**. Epigenetic and chromatin-based mechanisms in environmental stress adaptation and stress memory in plants. *Genome Biology* **18**: 1-11.

Langmead B, Trapnell C, Pop M, Salzberg SL. **2009**. Ultrafast and memory-efficient alignment of short DNA sequences to the human genome. *Genome biology* **10**: R25.

Leng X, Ivanov M, Kindgren P, Malik I, Thieffry A, Sandelin A, Kaplan CD, Marquardt S, Plant C, Centre S, *et al.* 2020. Organismal benefits of transcription speed control at gene boundaries. *EMBO reports* **21**: e49315.

Li S, Wang Y, Zhao Y, Zhao X, Chen X, Gong Z. **2020**. Global co-transcriptional splicing in Arabidopsis and the correlation with splicing regulation in mature RNAs. *Molecular Plant* **13**: 266-277.

Luco RF, Pan Q, Tominaga K, Blencowe BJ, Pereira-Smith OM, Misteli T. **2010**. Regulation of alternative splicing by histone modifications. *Science* **327**: 996–1000.

Marquez Y, Höpfler M, Ayatollahi Z, Barta A, Kalyna M. **2015**. Unmasking alternative splicing inside protein-coding exons defines exitrons and their role in proteome plasticity. *Genome Research* **25**: 995–1007.

Nojima T, Gomes T, Grosso ARF, Kimura H, Dye MJ, Dhir S, Carmo-Fonseca M, Proudfoot NJ. **2015**. Mammalian NET-seq reveals genome-wide nascent transcription coupled to RNA processing. *Cell* **161**: 526-540.

Nojima T, Rebelo K, Gomes T, Grosso AR, Proudfoot NJ, Carmo-Fonseca M. **2018**. RNA Polymerase II Phosphorylated on CTD Serine 5 Interacts with the Spliceosome during Co-transcriptional Splicing. *Molecular Cell* **72**: 369-379.

Patro R, Duggal G, Love MI, Irizarry RA, Kingsford C. **2017**. Salmon provides fast and bias-aware quantification of transcript expression. *Nature Methods* **14**: 417-419.

Ramírez F, Dündar F, Diehl S, Grüning BA, Manke T. **2014**. DeepTools: A flexible platform for exploring deep-sequencing data. *Nucleic Acids Research* **42**: W187-W191.

Reddy ASN, Marquez Y, Kalyna M, Barta A. **2013**. Complexity of the alternative splicing landscape in plants. *The Plant cell* **25**: 3657–83.

Reed R, Maniatis T. **1985**. Intron sequences involved in lariat formation during pre-mRNA splicing. *Cell* **41**: 95-105.

Roy D, Paul A, Roy A, Ghosh R, Ganguly P, Chaudhuri S. **2014**. Differential acetylation of histone H3 at the regulatory region of OsDREB1b promoter facilitates chromatin remodelling and transcription activation during cold stress. *PLoS ONE* **9**: e100343.

Sibley CR, Blazquez L, Ule J. **2016**. Lessons from non-canonical splicing. *Nature Reviews Genetics* **17**: 407–421.

Staiger D, Simpson GG. **2015**. Enter exitrons. *Genome Biology* **16**: 1-3.

Tilgner H, Knowles DG, Johnson R, Davis CA, Chakrabortty S, Djebali S, Curado J, Snyder M, Gingeras TR, Guigó R. **2012**. Deep sequencing of subcellular RNA fractions shows splicing to be predominantly co-transcriptional in the human genome but inefficient for lncRNAs. *Genome Research* **22**: 1616–1625.

Trincado JL, Entizne JC, Hysenaj G, Singh B, Skalic M, Elliott DJ, Eyras E. **2018**. SUPPA2: Fast, accurate, and uncertainty-aware differential splicing analysis across multiple conditions. *Genome Biology* **19**: 1-11.

Ullah F, Hamilton M, Reddy ASN, Ben-Hur A. **2018**. Exploring the relationship between intron retention and chromatin accessibility in plants. *BMC Genomics* **19**: 21-32.

Yu X, Meng X, Liu Y, Wang X, Wang TJ, Zhang A, Li N, Qi X, Liu B, Xu ZY. **2019**. The chromatin remodeler ZmCHB101 impacts alternative splicing contexts in response to osmotic stress. *Plant Cell Reports* **38**: 131–145.

Zhang R, Calixto C, Marquez Y, Venhuizen P. **2016**. AtRTD2: A Reference Transcript Dataset for accurate quantification of alternative splicing and expression changes in Arabidopsis thaliana RNA-seq data. *BioRxiv*: 051938.

Zhang R, Calixto CPG, Marquez Y, Venhuizen P, Tzioutziou NA, Guo W, Spensley M, Entizne JC, Lewandowska D, Have S Ten, *et al.* 2017. A high quality Arabidopsis transcriptome for accurate transcript-level analysis of alternative splicing. *Nucleic Acids Research* **45**: 5061-5073.

Zhang Q, Oh DH, DiTusa SF, RamanaRao M V., Baisakh N, Dassanayake M, Smith AP. **2018**. Rice nucleosome patterns undergo remodeling coincident with stress-induced gene expression. *BMC Genomics* **19**: 1–16.

Zhu JK. **2016**. Abiotic stress signaling and responses in plants. *Cell* **167**: 313–324.

Zhu J, Liu M, Liu X, Dong Z. **2018**. RNA polymerase II activity revealed by GRO-seq and pNET-seq in Arabidopsis. *Nature Plants* **4**: 1112-1123.

Zhu D, Mao F, Tian Y, Lin X, Gu L, Gu H, Qu L, Wu Y, Wu Z. **2020**. The features and regulation of co-transcriptional splicing in Arabidopsis. *Molecular Plant* **13**: 278-294.

Figure Legends

Fig. 1 Cold-induced changes in gene expression, alternative splicing, and nucleosome occupancy. **(a)** Venn diagram displaying the overlap between DEGs and DAS genes. **(b)** Histogram representing the number of DAS events detected in Arabidopsis RNA-seq data upon cold stress. **(c)** Venn diagram displaying the overlap between DAS genes and the genes detected within the differentially positioned nucleosome regions. DEGs and DAS are differentially expressed and alternatively spliced, genes, respectively. DNPs and DNPs-Genes are differentially positioned nucleosomes and the genes associated with them, respectively. The *p*-value (hypergeometric test) relates to the significance of overlap. A5'SS: Alternative 5' splice site, A3'SS: Alternative 3' splice site, IR: Intron retention events without exitrons, MX: Mutually exclusive exons, ES: Skipped exon, AF: Alternative first exon, EI: Exitrons, and AL: Alternative last exon.

Fig. 2 Association of nucleosome occupancy with different AS events and their different ratios. **(a)** The association of nucleosome occupancy with different AS events. The x-axis is the position relative to the acceptor site (left) and donor site (right); the y-axis is the average of nucleosome signal for the selected genomic regions. ANOVA-test has been performed to detect the significance of differential nucleosome occupancy around acceptor site ($p = 0.015$) and donor site ($p = 0.039$) of different AS events of Col-0 at 22^{o}C, and the donor ($p = 0.0138$) and the acceptor sites ($p = 0.0196$) of different AS events of Col-0 at 4^{o}C (b) Nucleosome profiles for different types of AS events grouped based on their PSI. ANOVA-test has been performed to detect significance of differential nucleosome occupancy of different PSI groups for of Col-0 at 22^{o}C and 4^{o}C, respectively; around the acceptor site of A3'SS ($p = 0.0129$, $p = 0.00112$), A5'SS ($p = 0.00033$, $p = 0.0112$), ES ($p = 0.000129$, $p = 0.00234$), and IR ($p = 0.00236$, $p = 0.132$), events. The x-axis is the position relative to the acceptor site; the y-axis is the average of nucleosome signal. ES: Exon skipping, A3'SS: Alternative 3'SS, A5'SS: Alternative 5'SS, and IR: Intron retention. Constitutive exons or introns are coloured in yellow, whereas exons/introns involved in the splicing event are coloured in blue. Curved lines indicate a splicing event. Red arrow pointing towards differences in scaling used to plot nucleosome profiles for 22^{o}C and 4^{o}C. Blue arrows indicate regions with significant changes in nucleosome occupancy.

Fig. 3 Profiles of nucleosome occupancy across DAS, non-DAS exons and alternatively spliced junctions. **(a)** Nucleosome profiles are plotted against the DAS and non-DAS exons with 500 bp upstream and downstream at 22^{o}C (left) and 4^{o}C (right), respectively. Nucleosome signal data were used in one-tailed *t* test, which confirmed that DAS exons has lower nucleosome occupancy compared to non-DAS exons at 22^{o}C and 4^{o}C ($p = 4.31977E^{-16}$) drops across DAS exons upon temperature shift ($p = 5.32124E^{-18}$), and that nucleosome occupancy profiles around DAS exons are different between Col-0 22^{o}C and 4^{o}C ($p = 1.05564E^{-65}$). The x-axis represents DAS/non-DAS exons scaled to 500 bp and their upstream and downstream flanking regions (500 bp); the y-axis represents the average nucleosome signal in the selected genomic regions. **(b)** Chart illustrating the number of AS junctions that are unaffected, positively or negatively affected. Percentages are calculated relative to the significant (*p*-value <0.05) AS detected by SUPPA **(c)** Average nucleosome occupancy level across donor (left) and acceptor (right) regions of all splicing junctions which are unaffected, positively, or negatively affected by cold stress. One-way ANOVA test show the significance of the differences in nucleosome occupancy for the different types of SJs around the donor ($p = 0.00813$; Col-0 22^{o}C, $p = 0.0206$;

Col-0 4°C) and the acceptor (p = 0.0293; Col-0 22°C, p = 0.00733, Col-0 4°C). Red arrow pointing towards differences in scaling used to plot nucleosome profiles for 22°C and 4°C. Blue arrows indicate regions with significant changes in nucleosome occupancy.

Fig. 4 Nucleosome profiles across exitrons and their flanking regions. **(a)** Nucleosome profiles across exitrons and -500/+500 bp flanking regions. Nucleosome signal data collected across exitrons were used in one-tailed *t* test, which confirmed that nucleosome signal across exitrons drops significantly at 4°C (p = 5.51E^{-127}). **(b)** Nucleosome profiles for exitrons grouped according to their Percent Spliced In (PSI) values. The x-axis is the position relative to exitrons, where EIs and EIe are exitron start and end, respectively; the y-axis is the average nucleosome signal. **(c)** Nucleosome occupancy across exitrons, retained introns, constitutively spliced introns, and their -500/+500 bp flanking regions in each sample. One-way ANOVA test has been performed to confirm the significance of the differences in nucleosome occupancy between constitutively spliced introns, exitrons, and IR^{-EI} at 22°C (p = 5.99e^{-09}) and 4°C (p = 1e^{-09}). IR^{-EI} - retained introns excluding exitrons, S and E - start and end of exitrons or retained/constitutive introns. Red arrow pointing towards differences in scaling used to plot nucleosome profiles for 22°C and 4°C. Blue arrows indicate regions with significant changes in nucleosome occupancy.

Supporting Information

Supporting Information Method S1 Details of the experimental procedure.

Fig. S1 GO term enrichment analysis of differentially expressed genes (DEGs) and differentially alternatively spliced (DAS) genes. The x-axis represents the -log10 FDR (significant FDR <0.05) value for GO term; the y-axis represents terms in biological processes (yellow), cellular components (blue), and molecular functions (green).

Fig. S2 Distribution of the mean changes in Percent Spliced In (PSI) values along with the expression of different AS transcripts. The x-axis is the average transcript abundance; the y-axis is the Delta PSI (ΔPSI) detected by SUPPA. Blue and grey dots represent significant (p-value < 0.05) and non-significant events (p-value > 0.05), respectively. ASE: all splicing events; EI: exitron splicing events; IR-EI: intron retention events excluding exitrons; IR: intron retention; A3'SS: alternative 3' splice site; A5'SS: alternative 5'SS; ES: exon skipping.

Fig. S3 Genome-wide representation of nucleosome occupancy levels displaying a drop in nucleosome signal across exons and flanking regions. The x-axis represents exons scaled to 500 bp and their upstream and downstream flanking regions (500 bp); the y-axis represents the average nucleosome signal level.

Table S1 Differentially expressed (DE) and differentially alternatively spliced (DAS) genes identified in Arabidopsis thaliana upon exposure to cold stress.

Table S2 Event coordinates extracted from AtRTDv2 annotation file using SUPPA as well as the percentage spliced in (PSI) of each event in different samples.

Table S3 Significant (p-value ≤0.05) differential splicing events for local alternative splicing events (ΔPSI value) detected by SUPPA.

533 **Table S4** List of nucleosomes detected by iNPS in Col-0 at 22°C and 4°C on Chromosomes 1-
534 5.

535 **Table S5** Differential nucleosome positioning analysis performed by SUPPA and iNPS.

536 **Table S6** Genes associated with windows enriched with the differentially positioned
537 nucleosomes.

538 **Table S7** Splice Junctions (SJs) grouped into positively, negatively, and unaffected SJs.

539

Fig. 1

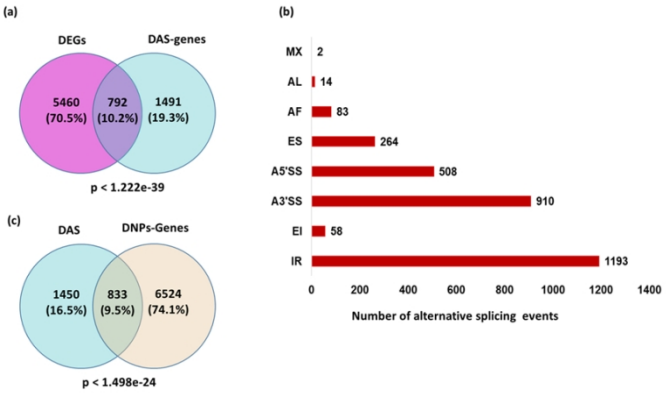

Fig. 1 Cold-induced changes in gene expression, alternative splicing, and nucleosome occupancy. (a) Venn diagram displaying the overlap between DEGs and DAS genes. (b) Histogram representing the number of DAS events detected in Arabidopsis RNA-seq data upon cold stress. (c) Venn diagram displaying the overlap between DAS genes and the genes detected within the differentially positioned nucleosome regions. DEGs and DAS are differentially expressed and alternatively spliced, genes, respectively. DNPs and DNPs-Genes are differentially positioned nucleosomes and the genes associated with them, respectively. The p-value (hypergeometric test) relates to the significance of overlap. A5'SS: Alternative 5' splice site, A3'SS: Alternative 3' splice site, IR: Intron retention events without exitrons, MX: Mutually exclusive exons, ES: Skipped exon, AF: Alternative first exon, EI: Exitrons, and AL: Alternative last exon.

338x190mm (96 x 96 DPI)

Fig. 2

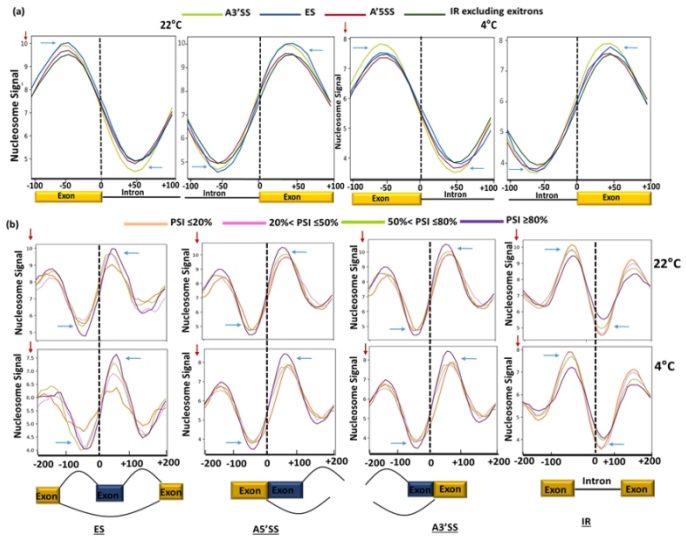

Fig. 2 Association of nucleosome occupancy with different AS events and their different ratios. (a) The association of nucleosome occupancy with different AS events. The x-axis is the position relative to the acceptor site (left) and donor site (right); the y-axis is the average of nucleosome signal for the selected genomic regions. ANOVA-test has been performed to detect the significance of differential nucleosome occupancy around acceptor site ($p = 0.015$) and donor site ($p = 0.039$) of different AS events of Col-0 at 22oC, and the donor ($p = 0.0138$) and the acceptor sites ($p = 0.0196$) of different AS events of Col-0 at 4oC (b) Nucleosome profiles for different types of AS events grouped based on their PSI. ANOVA-test has been performed to detect significance of differential nucleosome occupancy of different PSI groups for of Col-0 at 22oC and 4oC, respectively; around the acceptor site of A3'SS ($p = 0.0129$, $p = 0.00112$), A5'SS ($p = 0.00033$, $p = 0.0112$), ES ($p = 0.000129$, $p = 0.00234$), and IR ($p = 0.00236$, $p = 0.132$), events. The x-axis is the position relative to the acceptor site; the y-axis is the average of nucleosome signal. ES: Exon skipping, A3'SS: Alternative 3'SS, A5'SS: Alternative 5'SS, and IR: Intron retention. Constitutive exons or introns are coloured in yellow, whereas exons/introns involved in the splicing event are coloured in blue. Curved lines indicate a splicing event. Red arrow pointing towards differences in scaling used to plot nucleosome profiles for 22oC and 4oC. Blue arrows indicate regions with significant changes in nucleosome occupancy.

338x190mm (96 x 96 DPI)

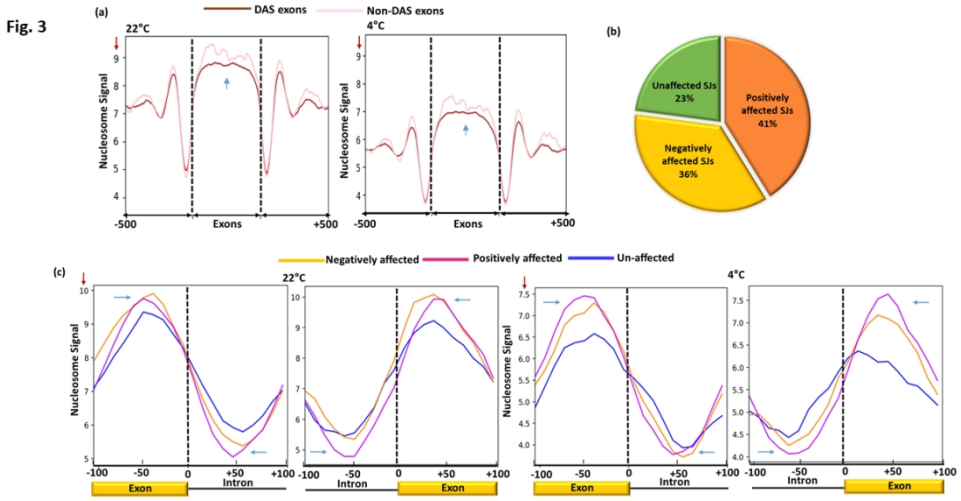

Fig. 3 Profiles of nucleosome occupancy across DAS, non-DAS exons and alternatively spliced junctions. (a) Nucleosome profiles are plotted against the DAS and non-DAS exons with 500 bp upstream and downstream at 22oC (left) and 4oC (right), respectively. Nucleosome signal data were used in one-tailed t test, which confirmed that DAS exons has lower nucleosome occupancy compared to non-DAS exons at 22oC and 4oC ($p = 4.31977E-16$) drops across DAS exons upon temperature shift ($p = 5.32124E-18$), and that nucleosome occupancy profiles around DAS exons are different between Col-0 22oC and 4oC ($p = 1.05564E-65$). The x-axis represents DAS/non-DAS exons scaled to 500 bp and their upstream and downstream flanking regions (500 bp); the y-axis represents the average nucleosome signal in the selected genomic regions. (b) Chart illustrating the number of AS junctions that are unaffected, positively or negatively affected. Percentages are calculated relative to the significant (p-value <0.05) AS detected by SUPPA (c) Average nucleosome occupancy level across donor (left) and acceptor (right) regions of all splicing junctions which are unaffected, positively, or negatively affected by cold stress. One-way ANOVA test show the significance of the differences in nucleosome occupancy for the different types of SJs around the donor ($p = 0.00813$; Col-0 22oC, $p = 0.0206$; Col-0 4oC) and the acceptor ($p = 0.0293$; Col-0 22oC, $p = 0.00733$, Col-0 4oC). Red arrow pointing towards differences in scaling used to plot nucleosome profiles for 22oC and 4oC. Blue arrows indicate regions with significant changes in nucleosome occupancy.

338x190mm (96 x 96 DPI)

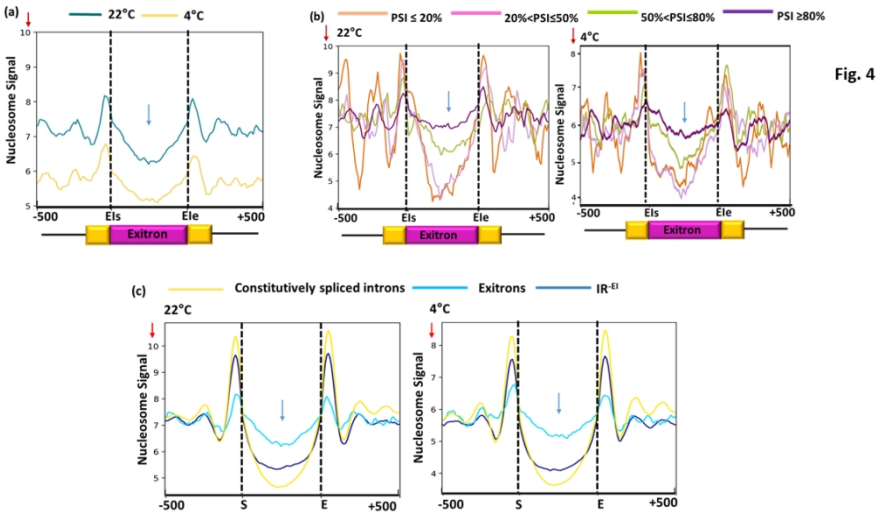

Fig. 4

Fig. 4 Nucleosome profiles across exitrons and their flanking regions. (a) Nucleosome profiles across exitrons and -500/+500 bp flanking regions. Nucleosome signal data collected across exitrons were used in one-tailed t test, which confirmed that nucleosome signal across exitrons drops significantly at 4oC ($p = 5.51E-127$). (b) Nucleosome profiles for exitrons grouped according to their Percent Spliced In (PSI) values. The x-axis is the position relative to exitrons, where EIs and EIe are exitron start and end, respectively; the y-axis is the average nucleosome signal. (c) Nucleosome occupancy across exitrons, retained introns, constitutively spliced introns, and their -500/+500 bp flanking regions in each sample. One-way ANOVA test has been performed to confirm the significance of the differences in nucleosome occupancy between constitutively spliced introns, exitrons, and IR-EI at 22oC ($p = 5.99e-09$) and 4oC ($p = 1e-09$). IR-EI - retained introns excluding exitrons, S and E - start and end of exitrons or retained/constitutive introns. Red arrow pointing towards differences in scaling used to plot nucleosome profiles for 22oC and 4oC. Blue arrows indicate regions with significant changes in nucleosome occupancy.

338x190mm (96 x 96 DPI)